

A mechanical model for the seismic vulnerability assessment of old masonry buildings

Luisa Carlotta Pagnini¹, Romeu Vicente², Sergio Lagomarsino^{1*} and Humberto Varum²

¹*Department of Civil, Environmental and Architectural Engineering - DICAT, University of Genova, Italy*

²*Department of Civil Engineering - DECIVIL, University of Aveiro, Portugal*

(Received June 9, 2010, Accepted November 29, 2010)

Abstract. This paper discusses a mechanical model for the vulnerability assessment of old masonry building aggregates that takes into account the uncertainties inherent to the building parameters, to the seismic demand and to the model error. The structural capacity is represented as an analytical function of a selected number of geometrical and mechanical parameters. Applying a suitable procedure for the uncertainty propagation, the statistical moments of the capacity curve are obtained as a function of the statistical moments of the input parameters, showing the role of each one in the overall capacity definition. The seismic demand is represented by response spectra; vulnerability analysis is carried out with respect to a certain number of random limit states. Fragility curves are derived taking into account the uncertainties of each quantity involved.

Keywords: capacity spectrum; fragility curves; uncertainties; damage assessment; seismic vulnerability.

1. Introduction

Seismic vulnerability assessment and damage scenarios at an urban scale are usually based on macroseismic or mechanical methods (Lagomarsino and Giovinazzi 2006). The former make use of macroseismic intensity hazard maps and give an estimate of the expected damage once the typology has been recognized among a given building catalogue. The latter simulate the structural capacity by mechanical models and represent the hazard scenarios in terms of peak ground acceleration or spectral values. Even within this approach, *in situ* observations of damages still represent a useful tool (D'Ayala 2005). In the class of mechanical methods, non-linear static procedures are gaining a central role (see for instance Cardone 2007 for a general frame) and have been adopted by most seismic codes for the design and the rehabilitation (EC8 2005). The capacity spectrum (Freeman 1998) is the main method used in ATC-40 (1996), while FEMA-273 (1997) refers to the displacement coefficient method; the main differences lie in the definition of inelastic seismic demand and lateral load pattern for the pushover analysis. The so called *N2* method is formulated as a modified capacity spectrum (Fajfar 1999) and is becoming very popular for its ready-to-use format.

In engineering practice, seismic verifications based on mechanical models usually assign structural

* Corresponding author, Professor, E-mail: sergio.lagomarsino@unige.it

parameters according to deterministic quantities, assumed on the basis of mean or nominal values. The analysis is carried out comparing deterministic values of the structural performance with deterministic limit states, according to criteria lacking a sound probabilistic procedure. The probability of exceeding a limit state is usually evaluated making use of all-inclusive empirical coefficients which take into account the uncertainties inherent in the structural capacity, seismic demand and limit states (HAZUS 1999). Even if this approach is justified by the difficulty in evaluating the actual variability of the quantities involved and by the need to provide simplified procedures for large scale analyses, it does not allow one to account for the actual uncertainties, which are different when dealing with a single building or with a group of buildings; nor to study the role of parameters and the propagation of the uncertainties involved, nor to account for the complete probabilistic features of the problem itself. Advanced formulations define earthquake loss giving a probabilistic description of building capacity, damage limit states and seismic demand. In the field of displacement based procedures, Crowley *et al.* (2004) include a fully probabilistic treatment for reinforced concrete buildings and study the impact of uncertainties in the damage scenarios (Crowley *et al.* 2005). Once that the statistical moments of the uncertain quantities are defined, fragility curves are obtained by an integral solution. Simplified mechanical models for masonry are dealt with by Restrepo-Velez and Magenes (2004). Recently, several extended stochastic analyses have been performed for masonry in specific locations (Erberik 2008, Bal *et al.* 2008, Mallardo *et al.* 2008); non linear analyses are carried out by calculation tools or commercial codes. The generalization of results can be obtained performing extended Monte Carlo simulations (Rota *et al.* 2010).

This paper presents a procedure for the probabilistic damage scenario assessment of masonry buildings on a large scale. Starting from a non-linear mechanical model (Cattari *et al.* 2004), it is derived an analytical description of the capacity curve and damage thresholds for in-line positioned aggregates which leaves free a certain number of geometrical, mechanical and constructive parameters. Structural performance is assessed according to a probabilistic approach which takes into account the actual variability of the structural response and seismic demand. The first part of the paper derives the mechanical model and defines damage thresholds suitable for the definition of probabilistic analyses. The second part studies the role of the parameter uncertainties and derives the damage scenarios. The case study considers the historical city centre of Coimbra for which the authors avail of an extended database of the main building parameters.

The model validation has been developed in the ambit of a risk assessment research project and was carried out over an ancient Italian town recently shaken by an earthquake (Cattari *et al.* 2010, Lagomarsino *et al.* 2010).

2. Basic formulation

Nonlinear static procedures evaluate the maximum response of a structure by a Single Degree of Freedom (*SDOF*) system characterized by equivalent stiffness and mass. The capacity of the structure subjected to monotonic loading is represented by a global pushover force - displacement curve. For building applications, it is the base shear versus top-displacement obtained distributing the lateral load according to the fundamental mode shape and the mass. The capacity spectrum is the capacity curve of the equivalent *SDOF* transformed into spectral acceleration and displacement coordinates. The displacement demand, or performance point, is evaluated by comparing the spectral

seismic demand, represented by either highly damped or inelastic spectra, with the capacity spectrum. The seismic effects over buildings are related to different limit states defined by spectral displacement values.

2.1 Damage assessment

Let S_d be the performance point and L_k be the spectral displacement related to a k -th limit state. The failure event $P_{f,k}$ is the probability that S_d exceeds L_k : $P_{f,k} = P(S_d > L_k)$. It is given by

$$P_{f,k} = \int_0^{\infty} F_{L_k}(s_d) f_{S_d}(s_d) ds_d \quad (1)$$

where s_d is the state variable of S_d , F_{L_k} is the cumulative distribution function of L_k ; f_{S_d} is the probability density function of S_d

$$f_{S_d}(s_d) = \int_{\Omega} f_{S_d|P,D,\varepsilon}(S_d|p,d,e) f_P(p) f_D(d) f_{\varepsilon}(e) dedddp \quad (2)$$

where P, D are vectors listing the parameters of the structure and of the seismic demand and ε lists the other inherent random quantities, including the zero-mean model error; $f_{S_d|P,D,\varepsilon}$ is the density function of S_d conditioned by the occurrence of P, D, ε ; $f_P, f_D, f_{\varepsilon}$ are the joint density functions of P, D, ε ; p, d, e are the state variables of P, D, ε ; Ω is the co-domain of P, D, ε .

2.2 Fragility curves

The evaluation of the integral in Eq. (2) is quite difficult when the random quantities are more than two or three. Therefore recourse is made to simplified procedures that don't require the knowledge of the distributions of the variables nor the solution of a multi-fold integral.

The safety margin M_k related to the k -th damage limit state is defined as

$$M_k = \log(L_k/S_d) \quad (3)$$

where \log is the natural logarithm. It is usually accepted that S_d and L_k are lognormal random quantities, therefore $P_{f,k}$ is given by

$$P_{f,k} = \Phi \left[-\frac{E[M_k]}{\sqrt{V[M_k]}} \right] \quad (4)$$

where Φ is the cumulative distribution function of the normal reduced random variable (with zero mean and unit standard deviation), $E[.]$ and $V[.]$ indicate mean and variance.

In engineering practice, the conditional probability (4) for the actual displacement of exceeding a given k -th damage limit state is generally defined in the form of a fragility curve (FEMA 1997)

$$P[S_d|L_k] = \Phi \left[\frac{1}{\beta_k} \times \log\left(\frac{\bar{S}_d}{L_k}\right) \right]; \quad \beta_k = \sqrt{V \left[\log\left(\frac{S_d}{L_k}\right) \right]} \quad (5)$$

where the symbols \bar{S}_d , \bar{L}_k are mean values, or nominal values, of S_d and L_k ; β_k is the standard deviation of the safety margin expressed by Eq. (3) and quantifies the uncertainties involved. It may be convenient to express β_k as the sum of different contributions, such as

$$\beta_k = \sqrt{\beta_{k,P}^2 + \beta_{k,D}^2 + \beta_{k,\varepsilon}^2} \quad (6)$$

where $\beta_{k,P}$, $\beta_{k,D}$, $\beta_{k,\varepsilon}$ are related respectively to the parameter uncertainties, to the seismic demand and other randomness

$$\beta_{k,P}^2 = V[M_k]^{|\bar{D}, \bar{\varepsilon}|}, \quad \beta_{k,D}^2 = V[M_k]^{|\bar{P}, \bar{\varepsilon}|}, \quad \beta_{k,\varepsilon}^2 = V[M_k]^{|\bar{P}, \bar{D}|} \quad (7)$$

where the superscript $|\bar{m}, \bar{n}|$ denotes quantities calculated in the mean values of \mathbf{m}, \mathbf{n} (being $\bar{\mathbf{m}}, \bar{\mathbf{n}} = \bar{\mathbf{P}}, \bar{\mathbf{D}}, \bar{\varepsilon}$). Values for β_k and for its contributions are given for instance in FEMA-273 (1997).

2.3 Approximate evaluation

Let $W = W(\mathbf{R})$ be a quantity depending on a vector \mathbf{R} of random parameters. The mean value-Taylor Series Expansion (*TSE*) develops W around the mean value of \mathbf{R} . Expanding up to the first order and applying the mean and variance operators to $W(\mathbf{R})$, one obtains

$$E[W] \simeq W(\bar{\mathbf{R}}), \quad V[W] \simeq \sum_i \sum_j \left. \frac{\partial W}{\partial R_i} \right|_{\bar{\mathbf{R}}} \left. \frac{\partial W}{\partial R_j} \right|_{\bar{\mathbf{R}}} Cov[R_i, R_j] \quad (8)$$

where: R_i, R_j are the i, j -th terms of \mathbf{R} ; $\bar{\mathbf{R}}$ is a vector listing the mean values \bar{R}_i of terms R_i ; the superscript $|\bar{\mathbf{R}}|$ denotes quantities evaluated in $\bar{\mathbf{R}}$, $Cov[.]$ indicates the covariance.

The Response Surface (*RS*) technique approximates the original, whatever complicated function $W(\mathbf{R})$ with a simpler, more computationally tractable polynomial. Using a first order polynomial and applying statistical operators to W , one has

$$E[W] \simeq v_0 + \sum_i v_i \bar{R}_i; \quad V[W] \simeq \sum_{ij} v_i v_j Cov[R_i, R_j] \quad (9)$$

where v_0, v_i, v_j are polynomial constants, the determination of which is accomplished through a least square regression fitting W at a sequence of sampling points in the neighbourhood of a nominal one, usually the mean value $\bar{\mathbf{R}} = \{\bar{R}_1, \bar{R}_2, \dots\}^T$.

The *RS* technique is suitable for numerical solutions or when facing with very time consuming functions to evaluate. Even if *TSE* requires the evaluation of the partial derivatives of the original function, it may be implemented through symbolic calculation tools when the structural response model is analytical.

3. Mechanical model

This paper deals with in-line historical building aggregates characterized by transversal walls with regular openings along the height and large openings in the façades along the longitudinal direction at ground floor (Fig. 1(a)). Two behaviour structural mechanisms can be found: *i*) uniform collapse

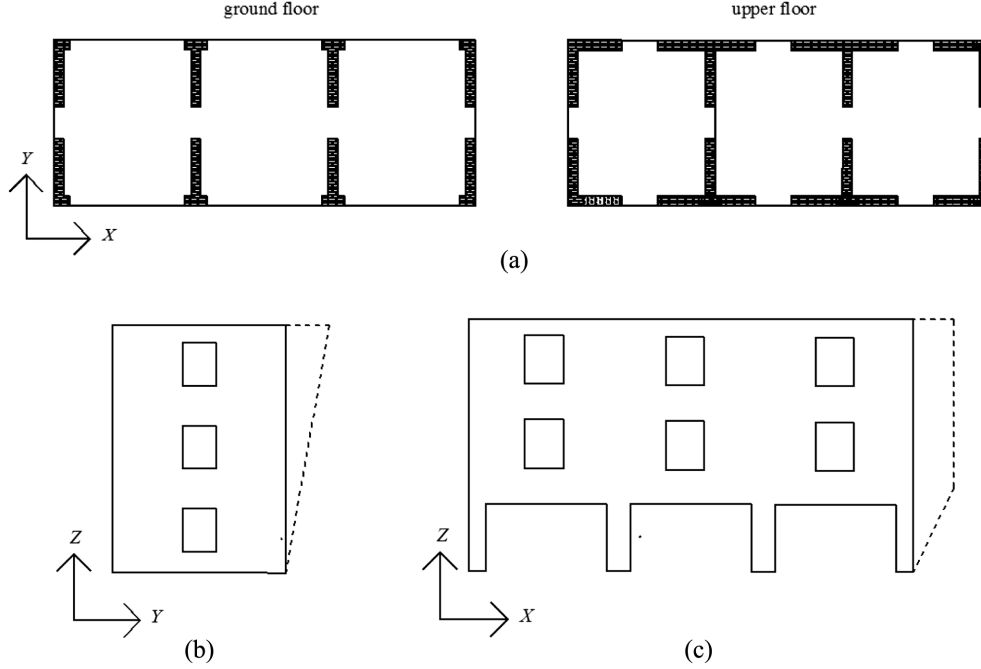


Fig. 1 In-line building aggregates: (a) building plans, (b) uniform mechanism, (c) soft-storey mechanism

mechanism (Fig. 1(b)), when the deformation and damage are distributed throughout the total height of the building and in the spandrels, *ii*) soft-storey mechanism in which the deformation demand is concentrated at the ground floor level (Fig. 1(c)).

3.1 Structural scheme

Let's consider a N -storey masonry building. It is represented by the stick model of height H with vertical axis coincident with axis Z ; X is coincident with the longitudinal direction, parallel with main plan dimension, Y is coincident with the transversal direction. The model, shown in Fig. 2(a), is clamped at the base and is described by N nodes above the ground, which shift position without rotating. Each node i is characterized by the lumped mass m_i at level $z_i = i \times h$, related to the i -th storey; $h = H/N$ is the inter-floor height. It has N elements, each i -th element is characterized by the area $A_{dir,i}$ and the inertia moment $J_{dir,i}$ of the resistant walls in the direction dir ; $dir = x$ is the direction parallel to X axis, $dir = y$ is parallel to Y axis. The structural response is related to the vector Ψ_{dir} which lists the N components $\psi_{dir,i}$ of the fundamental mode shape.

The equivalent $SDOF$ has an elastic perfectly plastic form. It represents a simplification of the actual pushover, obtained by suitable rules taking into accounts for the stiffness degradation and post peak branch.

The elastic vibration period in the direction considered is

$$T_{dir} = 2\pi \times \sqrt{M_{dir}^*/K_{dir}^*} \tag{10}$$

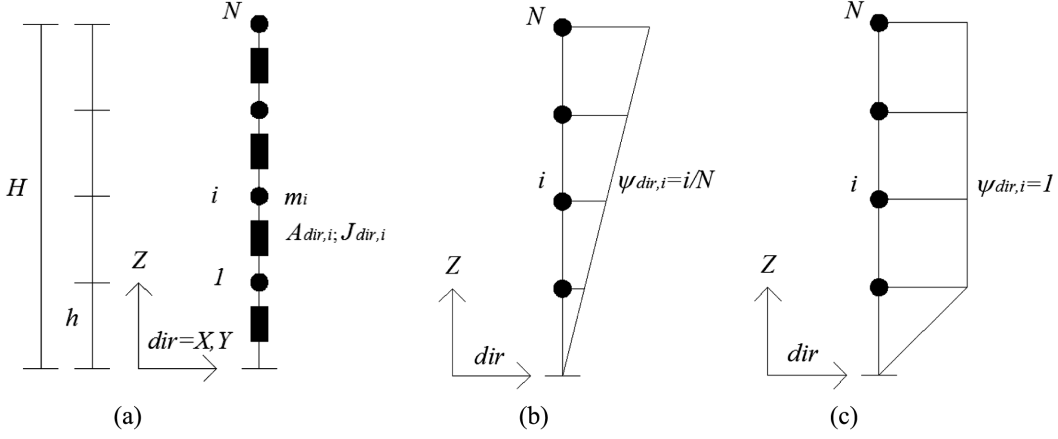


Fig. 2 (a) stick model, (b) uniform mechanism and (c) soft-storey mechanism

where M_{dir}^* is the equivalent generalized modal mass

$$M_{dir}^* = \sum_{i=1}^N m_i \times \psi_{dir,i}^2 \quad (11)$$

and K_{dir}^* is the equivalent generalized modal stiffness, which depends on the shear and flexural stiffness of the wall. The evaluation of this latter component requires a detailed definition of the resistant walls, which is hardly pursued during a quick building survey. This study relates the modal shape to the shear component only, which is prevailing in the building typology examined. It is given by

$$K_{dir}^* = h \sum_{i=1}^N G A_{dir,i} \times (\psi'_{dir,i})^2 \quad (12)$$

where $\psi'_{dir,i}$ is the i -th component of the prime derivative of the mode shape; G is the shear modulus. The yielding acceleration is given by

$$\alpha_{dir}^y = \frac{F_{dir}^y}{m_{dir}^* \times \Gamma_{dir}} \quad (13)$$

where F_{dir}^y is the yielding load of the building, m_{dir}^* is the equivalent mass, Γ_{dir} is the modal participation factor

$$m_{dir}^* = \sum_{i=1}^N m_i \times \psi_{dir,i}; \Gamma_{dir} = \frac{m_{dir}^*}{M_{dir}^*} \quad (14)$$

The yielding displacement d_{dir}^y is given by

$$d_{dir}^y = \frac{\alpha_{dir}^y}{(2\pi)^2} T_{dir} \quad (15)$$

For masonry buildings, F_{dir}^y is basically related to the shear strength of the walls at the ground floor level

$$F_{dir}^y = \xi \times A_{dir,1} \times \tau_{dir,u} \quad (16)$$

ξ being a coefficient which takes into account the non-uniform response of the masonry panels considered as shear driven mechanism, $\tau_{dir,u}$ is the ultimate base shear strength of the masonry (Turnsek and Cacovic 1971)

$$\tau_{dir,u} = \tau \times \sqrt{1 + \frac{\sigma_{dir,1}}{1.5 \times \tau}} \quad (17)$$

where τ is the reference shear strength ($\tau = f_t/1.5$, being f_t the tensile strength of the masonry) and $\sigma_{dir,1}$ is the compressive strength at the middle height of the first level masonry panels

$$\sigma_{dir,1} = \frac{\sum_{i=1}^N m_i \times g}{A_{dir,1}} \quad (18)$$

with g the gravity acceleration. The resistant wall area $A_{dir,i}$ for the direction considered is expressed as a function of the gross area A_p at top floor level in the same direction

$$A_{dir,i} = b_{dir,i} \times A_{dir,N} \text{ for } i = 1..N; A_{dir,N} = \alpha_{dir} \times A_p \quad (19)$$

where $b_{dir,i}$, α_{dir} are suitable coefficients. The i -th mass related to level i can be expressed as

$$m_i = (A_{x,i} + A_{y,i}) \times \gamma \times h + A_p \times q \quad (20)$$

where γ is the mass density of the masonry, q is the floor mass (related to permanent and live loads). The compressive strength, Eq. (18), can therefore be expressed as

$$\sigma_{dir,1} = g \times \gamma \times h \times \frac{\sum_{i=1}^N b_{dir,i}}{b_{dir,1}} + \frac{N \times q \times g}{\alpha_{dir} \times b_{dir,1}} \times \delta_{dir} \quad (21)$$

δ_{dir} being a Boolean type coefficient, $\delta_{dir} = 0$ or 1 depending on the path of the floor loading onto the masonry walls. When the loading path varies, it is an average value between 0 and 1.

The ultimate displacement of the bilinear capacity curve, d_{dir}^u , can be derived according to the collapse mode

$$d_{dir}^u = t_u \times \frac{N \times h}{\Gamma_{dir}} \text{ for a uniform collapse mode} \quad (22)$$

$$d_{dir}^u = t_u \times h + d_{dir}^y \times \left(1 - \frac{\Gamma_{dir}}{N}\right) \text{ for a soft storey collapse mode}$$

where t_u is the ultimate drift of the masonry panel, which depends on the masonry quality and

typology (EC8 2005).

On the basis of numerical simulations (Cattari *et al.* 2009), suitable coefficients can be applied to the strength and the stiffness to account for the flexural contribution to stiffness, for flexural failure mechanisms of piers, for irregularities in the pier distribution or in the plan configuration, for a failure mechanism related to the weak spandrels – strong piers condition, for irregularities in the case of flexible diaphragms.

The numerical validation of the mechanical model and the calibration of coefficients has been developed in the ambit of a risk assessment research program (Lagomarsino *et al.* 2010, Cattari *et al.* 2010) over the case of an ancient Italian town recently shaken by a severe earthquake.

3.2 Uniform mechanism

When the structure responds basically according to a uniform mode shape, the i -th component of the fundamental eigenvector is assumed to be linear, i.e. $\psi_{dir,i} = i/N$ (see Fig. 2(b)). The fundamental period of vibration and the yielding acceleration α_{dir}^y can be expressed by

$$T_{dir} = 2\pi \times \sqrt{\frac{h}{G \times \alpha_{dir} \times \sum_{i=1}^N b_{dir,i}} \times \left[\gamma \times h \left(\alpha_x \times \sum_{i=1}^N b'_{x,i} \times i^2 + \alpha_y \sum_{i=1}^N b'_{y,i} \times i^2 \right) + q \sum_{i=1}^N i^2 \right]} \quad (23)$$

$$\alpha_{dir}^y = \frac{\beta_{dir,1} \times \xi \times \tau \times \sqrt{1 + \frac{g}{1.5 \times \tau \times b_{dir,1}} \times \left(\gamma \times h \times \sum_{i=1}^N b_{dir,i} + \frac{N \times q \times \delta_{dir}}{\alpha_{dir}} \right)}}{\kappa} \quad (24)$$

being

$$\kappa = \frac{1}{\alpha_y} \times \frac{\left[\gamma \times h \times \left(\alpha_x \sum_{i=1}^N b'_{x,i} \times i + \alpha_y \sum_{i=1}^N b'_{y,i} \times i \right) + q \times \sum_{i=1}^N i \right]^2}{\gamma \times h \times \left(\alpha_x \sum_{i=1}^N b'_{x,i} \times i^2 + \alpha_y \sum_{i=1}^N b'_{y,i} \times i^2 \right) + q \times \sum_{i=1}^N i^2} \quad (25)$$

$$b'_{dir,i} = \frac{1}{2}(b_{dir,i} + b_{dir,i+1}) \text{ for } i = 1, \dots, N-1; \quad b'_{dir,N} = \frac{1}{2}b_{dir,N} \text{ for } i = N \quad (26)$$

the ultimate displacement d_{dir}^u is obtained by Eq. (22), where Γ_{dir} is given by

$$\Gamma_{dir} = N \times \frac{\gamma \times h \times \left(\alpha_x \sum_{i=1}^N b'_{x,i} \times i + \alpha_y \sum_{i=1}^N b'_{y,i} \times i \right) + q \times \sum_{i=1}^N i}{\gamma \times h \times \left(\alpha_x \sum_{i=1}^N b'_{x,i} \times i^2 + \alpha_y \sum_{i=1}^N b'_{y,i} \times i^2 \right) + q \times \sum_{i=1}^N i^2} \quad (27)$$

3.3 Soft-storey mechanism

When the structural behaviour is ruled by a soft storey mechanism, the modal displacement at upper levels is assumed to be constant, i.e. $\psi_i = 1$ (see Fig. 2(c)) and the resulting equations take a simpler layout. The fundamental vibration period and the yielding acceleration are given by

$$T_{dir} = 2\pi \times \sqrt{\frac{h}{G \times b_{dir,1} \times \alpha_{dir}} \left[h \times \gamma \times \left(a_x \sum_{i=1}^N b'_{x,i} + a_y \sum_{i=1}^N b'_{y,i} \right) + N \times q \right]} \quad (28)$$

$$\alpha_{dir}^y = \frac{b_{dir,1} \times \xi \times \tau \times \sqrt{1 + \frac{g}{1.5 \times \tau \times b_{dir,1}} \times \left(\gamma \times h \times \sum_{i=1}^N b_{dir,i} + \frac{N \times q \times \delta_{dir}}{\alpha_{dir}} \right)}}{\kappa} \times \frac{\alpha_{dir}}{\alpha_y} \quad (29)$$

with

$$\kappa = \gamma \times h \times \left(\frac{\alpha_x}{\alpha_y} \sum_{i=1}^N b'_{x,i} + \sum_{i=1}^N b'_{y,i} \right) + \frac{N \times q}{\alpha_y} \quad (30)$$

The ultimate displacement d_{dir}^u is obtained by Eq. (22); I_{dir} is equal to 1. The pedix $[\cdot]_{dir}$ is omitted from now on.

3.4 Wall area distribution

Expressions are herein derived for terms in Eqs. (23), (24), (28), (29) according to two different conditions of the wall resistant area distribution. The first condition applies when the resistant walls are characterized by large openings or disalignments at the first level. In this case a bilinear distribution is assumed (Fig. 3, solid line). The second condition applies when the resistant wall area, for the direction considered, decreases linearly on increasing the floor level (Fig. 3, dashed line). In both cases, coefficients b_i are expressed by

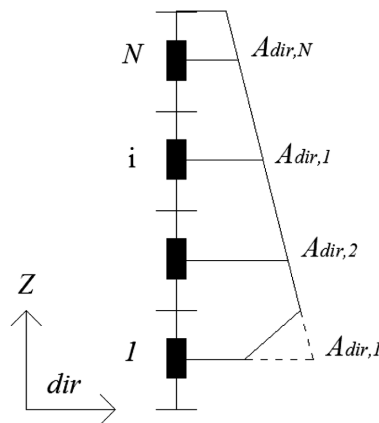


Fig. 3 Wall areas in height

$$\begin{aligned}
b_1 &= \text{to be assigned} \\
b_2 &= \begin{cases} \text{to be assigned in case of bi-linear wall area distribution} \\ \frac{1}{N-1} + b_1 \frac{N-2}{N-1} & \text{for linear wall area distribution} \end{cases} \quad (31) \\
b_i &= \frac{i-2}{N-2} + b_2 \frac{N-i}{N-2} \quad i = 3, \dots, N
\end{aligned}$$

For bilinear wall area distribution, Eq. (31) takes the form

$$\begin{aligned}
\sum_{i=1}^N b_i &= b_1 + \frac{1}{N-2} \left[(N-1)(b_2 N - 2) + (1-b_2) \sum_{i=2}^N i \right]; \quad \sum_{i=1}^N b'_i = \sum_{i=1}^N b_i - \frac{b_1}{2} \\
\sum_{i=1}^N b'_i \times i &= \frac{1}{2} + \frac{1}{2(N-2)} \left[2(1-b_2) \sum_{i=2}^N i^2 + (b_2 - 5 + 2N \times b_2) \sum_{i=2}^N i + (N-1)(2-Nb_2) \right] \quad (32) \\
\sum_{i=1}^N b'_i \times i^2 &= \frac{b_1}{2} + \frac{1}{2(N-2)} \left[2(1-b_2) \sum_{i=2}^N i^3 + (2b_2 - 6 + 2N \times b_2) \sum_{i=2}^N i^2 - (b_2 - 5 + 2N \times b_2) \sum_{i=2}^N i - (N-1)(2-Nb_2) \right]
\end{aligned}$$

For buildings characterized by a uniform distribution along the height, it can be rewritten as

$$\begin{aligned}
\sum_i b_i &= \frac{1}{N-1} \times \left[(Nb_1 - 1) \times N + (1-b_1) \times \sum_i i \right] \\
\sum_i b'_i \times i &= \frac{1}{2(N-1)} \times \left[(2Nb_1 - b_1 - 1) \times \sum_i i + 2(1-b_1) \times \sum_i i^2 - N(N-b_1) \right] \quad (33) \\
\sum_i b'_i \times i^2 &= \frac{1}{2(N-1)} \times \left[(2Nb_1 - b_1 - 1) \times \sum_i i^2 + 2(1-b_1) \times \sum_i i^3 - N^2(N-b_1) \right]
\end{aligned}$$

3.5 Limit states

The development of seismic damage over the building elements is represented, in global terms, by the progressive degradation of the pushover. The equivalent bilinear curve describes the main aspects of the problem, allowing to define, in a synthetic way, the entity and the extension of the damage by means of a displacement measure.

Damage levels are defined in terms of spectral displacement according to four limit states (HAZUS 1999): slight, moderate, extensive, complete. Slight damage indicates a condition still far from the reaching of the maximum strength and corresponds to local damage in few structural

elements. Moderate damage corresponds to the maximum value of the restoring force in the pushover curve, and is located, in terms of spectral displacement, after the yielding condition of the equivalent bilinear (this position comes out from the evaluation of the equivalent bilinear curve from the actual pushover curve). Complete damage is defined on the basis of the ultimate displacement conditions for structural walls. Extensive damage lies in an intermediate position. Limit states are defined by their probability density functions (Fig. 4)

$$\begin{cases} p_{L_k}(l_k) = \lambda_{L,k} & \text{for } \theta_{L,k} \leq l_k < \bar{L}_k \\ p_{L_k}(l_k) = \lambda_{U,k} & \text{for } \bar{L}_k \leq l_k < \theta_{U,k} \\ p_{L_k}(l_k) = 0 & \text{elsewhere} \end{cases} \quad (34)$$

where l_k is the state variable of L_k , \bar{L}_k is the mean or nominal value of the k -th limit displacement; $\theta_{L,k}$, $\theta_{U,k}$ are lower and upper bounds laying on the mean point between \bar{L}_k , \bar{L}_{k+1} . For the equivalent *SDOF*, the following expressions are suggested (Cattari *et al.* 2004)

$$\bar{L}_1 = 0.7d^y; \bar{L}_2 = 1.5d^y; \bar{L}_3 = 0.5 \times (d^y + d^u); \bar{L}_4 = d^u; \text{ being } d^u > 2d^y \quad (35)$$

$$\theta_{L,1} = 0.4d^y; \theta_{L,2} = d^y; \theta_{L,3} = d^y + 0.25d^u; \theta_{L,4} = 0.25(d^y + 3d^u)$$

$$\theta_{U,1} = d^y; \theta_{U,2} = d^y + 0.5d^u; \theta_{U,3} = 0.25(d^y + 3d^u); \theta_{U,4} = 1.3d^u$$

For any value of S_d , discrete damage-state probabilities can be calculated as the difference between the cumulative probabilities of reaching, or exceeding, successive damage states

$$P_{S,0} = 1 - P[L_1|S_d]; P_{S,k} = P[L_k|S_d] - P[L_{k+1}|S_d] \text{ for } k = 1, 2, 3; p_{S,4} = P[L_4|S_d] \quad (36)$$

where $p_{S,0}$ is the probability associated with no damage; $p_{S,k}$ is the probability that the damage

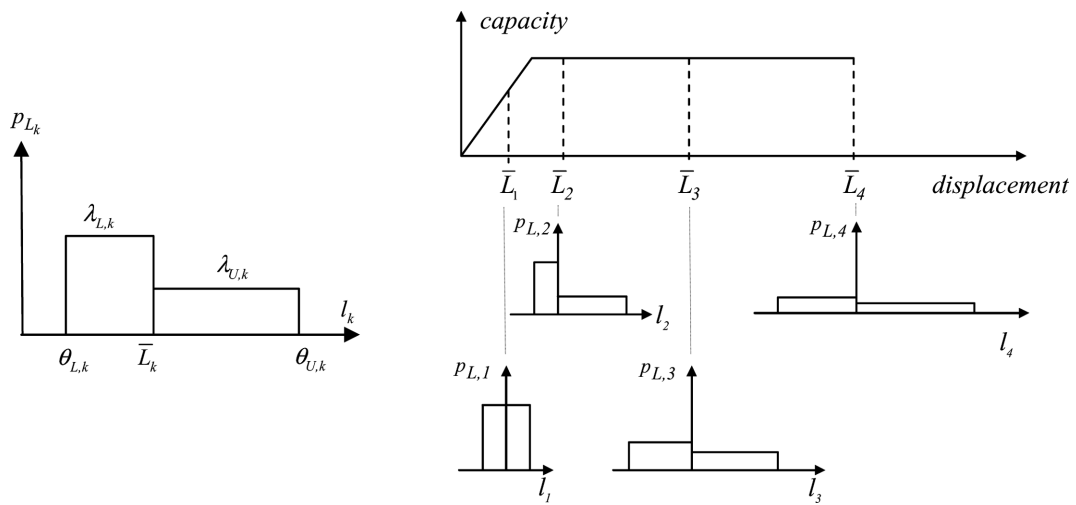


Fig. 4 Distribution of the damage limit states

scenario is within the k -th damage state, i.e. it exceeds the k -th limit and it is less than the $k+1$ -th one; $p_{S,4}$ is the probability that the building has reached the ultimate damage limit state.

4. Uncertainty propagation and damage assessment

Random quantities involved can be inherently random, such as the variability in parameters among the building stock, the model error, the seismic demand, the limit states, or they can be uncertain quantities, affected by errors due to lack of knowledge or simplifications. They can be classified according to the physical aspect they are ruling, such as the structural model, the seismic demand, other randomness, as expressed in Eq. (6). They can be classified in non cognitive (quantitative) and cognitive (qualitative) sources (Haldar and Mahadevan 2000). The former arise from: 1) the inherent randomness in physical observations, such as uncertainties in the experimental measures of mechanical and geometrical parameters; moreover, the seismic demand cannot be predicted by certainty, thus it is inherent random, 2) statistical uncertainties, due to the uncertainties in the variability of the physical quantities and 3) modelling uncertainties, inherent in the representation of the system behaviour. Cognitive uncertainties arise from the definition of qualitative quantities, such as limit states.

The definition of the mechanical model is affected by uncertainties due to the parameters and to the model itself. Parameter uncertainties are mainly due to the inherent randomness in the observations, to statistical errors due to the limited data when dealing with building stocks, to the model errors. For a single building, it is quite easy to obtain good estimates of the geometrical parameters $a_x, a_y, b_{x,b}, b_{y,b}, H$. The evaluation of mechanical parameters γ, τ, G requires the execution of experimental tests, yet, their evaluation is rather uncertain; very rough estimates can be obtained on the basis of a quick building survey. The loading path coefficient, δ , can be determined according to the structural scheme of the floor, even if the loading distribution is still random; randomness is inherent in q . The estimate of these quantities becomes unavoidably more scattered when dealing with building stocks. Uncertainties in threshold definition are even greater. The model error can be reduced by numerical validations, but the scattering of the estimates is very difficult to evaluate.

Using the analytical model illustrated above, statistical moments of a^y, T, L_k can be expressed by *TSE*, assuming $\mathbf{R} = \{\mathbf{P}^T, \boldsymbol{\varepsilon}^T\}^T$, where $\boldsymbol{\varepsilon}$ lists the model error and the inherent randomness in limit states. Using symbolic calculation tools, uncertainties can be propagated over the structural capacity by Eq. (8).

The evaluation of the damage scenarios requires the definition of the seismic demand and the choice of the calculation procedure. Different procedures are equivalent only in particular conditions and the errors committed are very large in many cases. The probabilistic assessment of the seismic demand can be dealt with in a different manner for vulnerability or risk analyses. Large uncertainties affect both the peak ground acceleration and the harmonic content; moreover, large spatial variability can be observed due to variation of the soil conditions or topography. Advanced seismic codes provide analytical response spectra for given return periods together with their variability.

Following the *N2* method, the procedure presented in the previous sections can be implemented analytically. In this case, M_k can be expressed by *TSE* as an analytical function of the building parameters \mathbf{P} , the seismic demand \mathbf{D} , and the other randomness $\boldsymbol{\varepsilon}$. Statistical moments of the margin

and fragility curves can be obtained by Eq. (8). When the margin is not analytical, i.e. the seismic demand is numerical or the performance point evaluation involves a numerical solution, damage assessment can be obtained by *RS*, using Eq. (9), or Monte Carlo simulations. In some cases, some steps of the solution can be carried out analytically and some others numerically. Therefore some contributions in Eq. (6) can be evaluated by Eq. (8) and others by Eq. (9).

5. Numerical application

5.1 Case study

In the ambit of the rehabilitation and refurbishment project for the old city centre of Coimbra, two of the authors of this paper have been involved in an accurate data collection of the basic information of the existing buildings (Vicente *et al.* 2006). The availability of this catalogue has represented an interesting chance to derive statistical information of the parameters and their correlations, and for the application of the methodology at a large scale.

Due to the particular evolution of the urban layout and to the chronological construction process, adjacent buildings share load-bearing masonry walls and their façade walls are aligned. The city plan reveals that they should be studied as aggregates in the longitudinal direction, where the wall area distribution suggests a soft storey mechanism, while they can be studied as independent units in the transversal direction.

The model herein discussed is applied to the transversal response (*dir* = *Y*) of the four-storey buildings in the old city centre (Fig. 5). The statistical analysis of the database, listing 77 cards, each related to one building unit, has furnished the following data: $E[h] = 2.9$ m, $E[b_{x,1}] = 1.2$, $E[b_{y,1}] = 1.0$, $E[\alpha_x] = 0.04$, $E[\alpha_y] = 0.07$, $Var[h] = 0.14$, $Var[b_{x,1}] = 0.38$, $Var[b_{y,1}] = 0.25$, $Var[\alpha_x] = 0.38$, $Var[\alpha_y] = 0.36$, being $Var[.] = \sqrt{V[.]/E[.]^2}$. The correlation coefficient of $b_{x,1}$, α_x and of $b_{y,1}$, α_y is equal to -0.5. The other parameters, not reported by the database, have been estimated as follows:

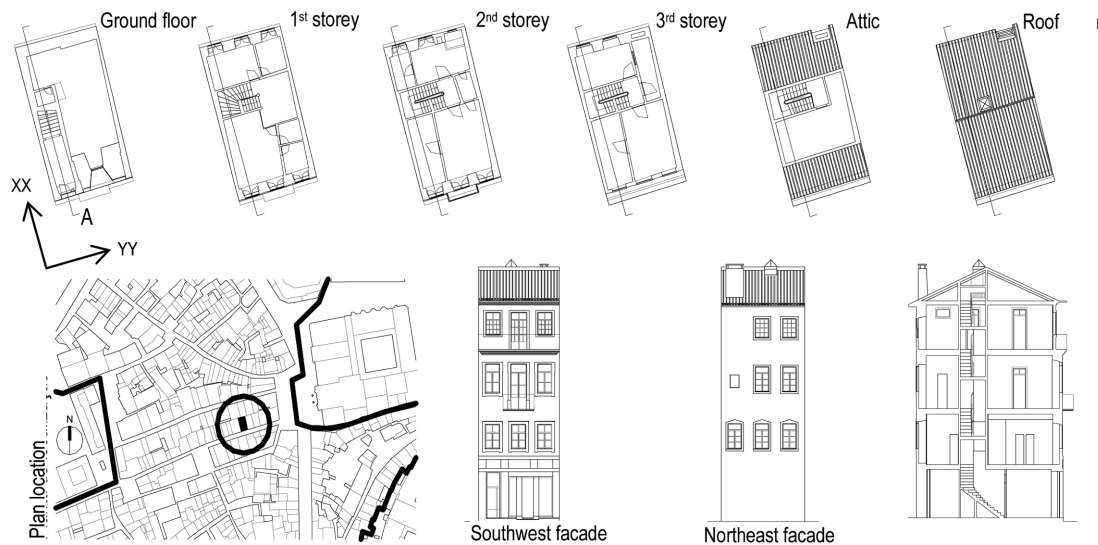


Fig. 5 A four storey building included in the data base

$E[q] = 400 \text{ kg/m}^2$, $E[\gamma] = 2200 \text{ kg/m}^3$, $E[G] = 2 \times 10^8 \text{ N/m}^2$, $E[\tau] = 90000 \text{ N/m}^2$. $\text{Var}[q] = 0.4$, $\text{Var}[\gamma] = 0.2$, $\text{Var}[G] = 0.2$, $\text{Var}[\tau] = 0.3$. These quantities are assumed uncorrelated. Moreover $\delta = 1$, $\xi = 1$, $t_u = 0.04$. In this example, the model error is not considered. The wall resistant areas decrease linearly along the height and a uniform collapse mode is expected.

5.2 Structural capacity

The first step propagates the uncertainties in $\mathbf{P} = \{h, b_{x,1}, b_{y,1}, \alpha_x, \alpha_y, q, \tau, \gamma, G\}^T$ over the building capacity curve by *TSE*. The pedix $[\cdot]_y$, which refers to the response direction, is omitted. The effects related to each term of \mathbf{P} are obtained by modelling in terms of random variables just one parameter at a time, taking the remaining ones as coincident with their means. Each time, first order approximations of the mean and variance of a quantity characterizing the capacity curve, i.e. $W = T, \alpha^y, d^u, L_1 \dots L_4$, are obtained by Eq. (8).

Fig. 6 shows the variability of the capacity curve (in the acceleration and displacement format)

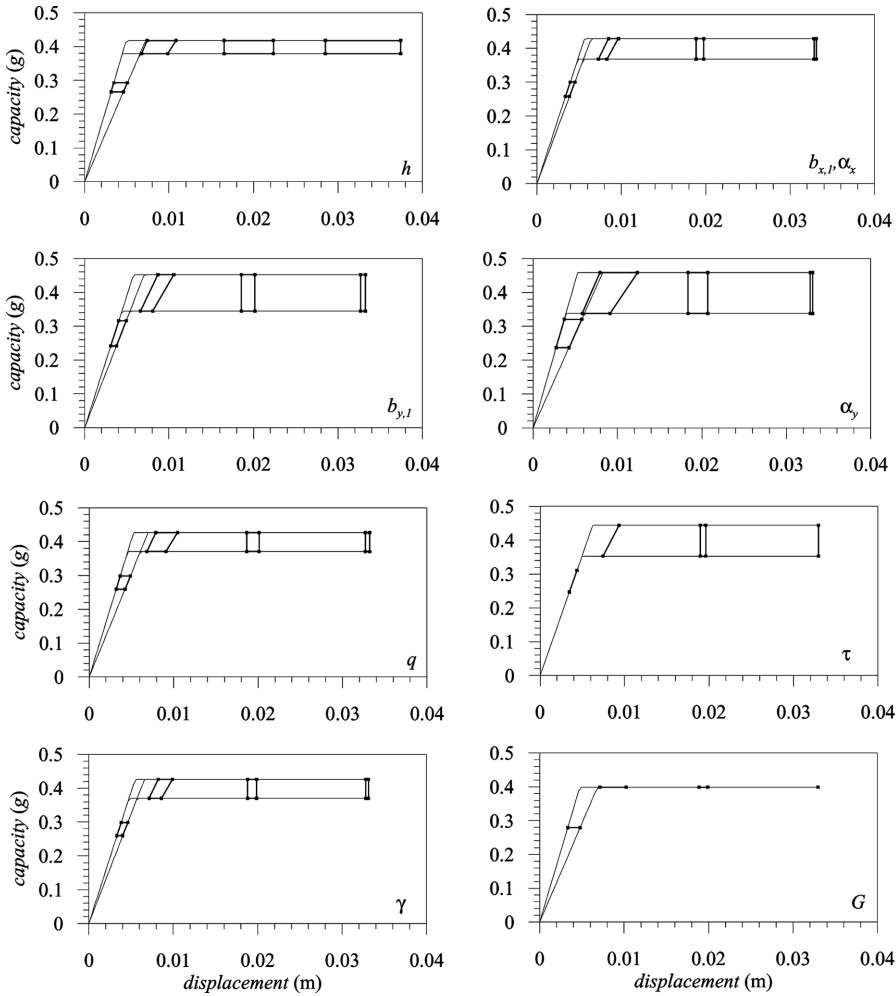


Fig. 6 Propagation of parameter uncertainties over the structural capacity

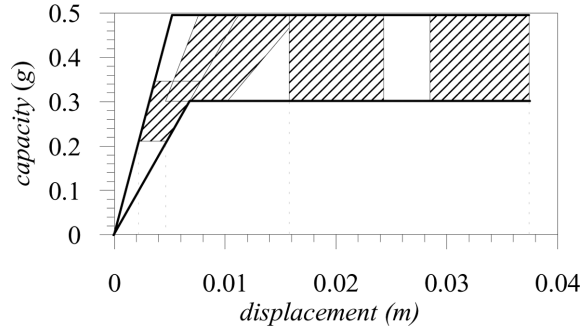


Fig. 7 Uncertainty propagation due to all parameters

and of the limit states associated to each term of \mathbf{P} . Parametric diagrams correspond to the mean value plus and minus a standard deviation. The scattering shown allows several comments concerning the uncertainty propagation of each parameter singularly and the implications on the results. Each parameter differently affects the period and the strength. The inter-storey height (h) is affected by small variability; the specific mass (γ) of the masonry and the floor mass play a secondary role, therefore rough estimates would not interfere much in the results. The shear modulus influences the elastic behaviour only; its role is expected to be small for heavy damages. Quantities α_x and $b_{x,1}$ are quite secondary for this direction, yet it is expected that their relevant scatter affects the longitudinal response. Overall, the parameters of resistant wall area, α_y and $b_{y,1}$ and the shear strength, τ are the most significant ones and they are at the mean time the ones endowed by the largest variability.

The effects associated with the uncertainties of all parameters in the capacity curve are shown in Fig. 7. Shaded areas represent the damage state variability. The average diagram is described by $E[T] = 0.24$ s, $E[\alpha^y] = 0.40$ g, $E[d^y] = 5.6 \times 10^{-3}$ m, $E[L_1] = 3.9 \times 10^{-3}$ m, $E[L_2] = 8.4 \times 10^{-3}$ m, $E[L_3] = 19 \times 10^{-3}$ m, $E[L_4] = 33 \times 10^{-3}$ m.

5.3 Vulnerability evaluation

Vulnerability is evaluated with respect to earthquake actions for return period of 475 years. The seismic demand is characterized by the elastic spectrum given by EC8 (2005) for soil type C; the expected peak ground acceleration (pga) is 0.2 g and its Var is assumed to be 0.15. This value does not represent the actual variability of the seismic action, but represents the variability averagely assigned by seismic codes to the pga for given return periods (see for instance <http://zonesismiche.mi.ingv.it/>).

For each limit state, fragility curves are determined by the following steps: 1) structural capacity and damage limit states are expressed as an analytical function of \mathbf{P} ; 2) the spectral displacement S_d is obtained according to the $N2$ analytical procedure; 3) the safety margin M_k is defined through Eq. (3) for each limit state. It is an analytical function of \mathbf{P} , \mathbf{D} , $\boldsymbol{\varepsilon}$; \mathbf{P} lists the random parameters of the structural models; \mathbf{D} represents the pga ; $\boldsymbol{\varepsilon}$ represents the inherent randomness of the limit states; it is obtained from Eqs. (34), (35), with the building parameters fixed. The mean value and standard deviation of M_k are obtained developing the marginal function in Taylor series. The exceeding threshold and damage state probabilities are obtained from Eqs. (4), (36); step 4) calculates the different contributions of β_k defined in Eq. (6). Figs. 8 and 9 show the fragility curves and the

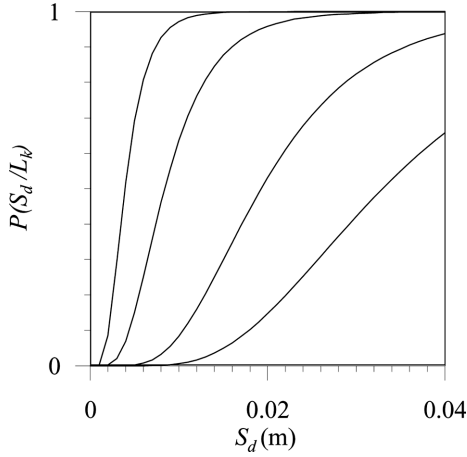


Fig. 8 Fragility curves

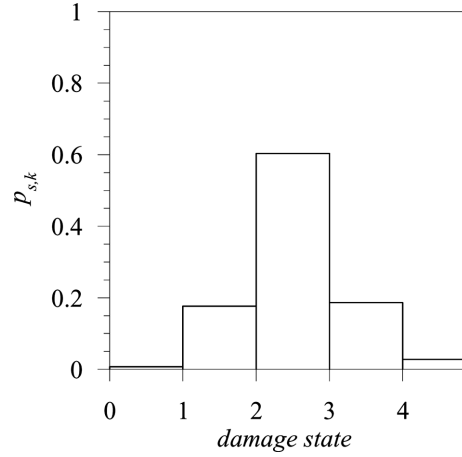


Fig. 9 Damage probabilities

Table 1 Margin variability and failure probability

limit state	1	2	3	4
$\beta_{k,P}$	0.35	0.35	0.37	0.38
$\beta_{k,D}$	0.25	0.25	0.25	0.25
$\beta_{k,\varepsilon}$	0.24	0.26	0.18	0.14
β_k	0.49	0.50	0.48	0.48
$P_{s,k}$	0.18	0.60	0.19	0.03
$P_{f,k}$	0.99	0.82	0.21	0.03

The performance point (mean value) is $E[S_d] = 0.013$ m

damage probabilities; Table 1 resumes the main results exposing the different contributions in the safety index due to parameters ($\beta_{k,P}$), *pga* ($\beta_{k,D}$), inherent randomness of limit states ($\beta_{k,\varepsilon}$) and gives the exceeding threshold probabilities. Other model errors have not been included in $\beta_{k,\varepsilon}$.

Values in Table 1 show that $\beta_{k,P}$ is the main contribution to β_k . Nevertheless, $\beta_{k,\varepsilon}$ and $\beta_{k,D}$ could become much higher when including other inherent randomness, such as errors in modeling, errors due to the procedure applied and variability in the seismic action. Preliminary risk analyses (Cattari *et al.* 2010), carried out taking into account the actual probabilistic characterization of the seismic event, have already shown that the damage scenario spreads up to the point of making parameter uncertainties almost negligible.

For the case study, the most probable damage scenarios turns out to be moderate.

6. Conclusions

This paper presents a probabilistic procedure of vulnerability and risk assessment suitable for analyses in historical centres, where a large number of old masonry buildings of different types and number of floors are present. Based on the use of a mechanical model, and leaving free the definition of the building parameters, of the limit states and of seismic demand, fragility curves

have been derived as a function of the uncertainties involved, allowing the discussion and interpretation of the different contributions. Availing of first order reliability methods, the formulation proposed can be easily applied on the basis of quick building surveys and can be implemented by symbolic calculation tools. According to the procedure adopted for the non linear analysis, the solution can be analytical or numerical. Also, it can be developed in a unitary way, or, alternatively, different steps and uncertainties can be processed by different approaches.

The numerical example is carried out in terms of vulnerability analysis in order to illustrate the mechanical model and the application of the procedure. From a numerical point of view, it does not account for some actual uncertainties, such as the model errors and the uncertainty in seismic event. The seismic demand is represented by a given response spectrum and its variability is characterized by the *pga* variability, estimated for a given return period. Results show the scattering of the capacity curve due to the uncertainties of the model parameter and show the different contributions on the overall damage scenarios due to building parameters, seismic demand, inherent randomness in limit states. Here they are almost comparable. This fact, even if it is strictly related to the case study, reveals that the role of uncertainties in the building stock parameters is likely to become negligible when including model errors and the probabilistic description of the seismic event, which is crucial for a proper risk analysis. At this purpose, the authors are working in collaboration with geophysics researchers at a probabilistic characterization of the response spectra by simulating the fault rupture which is expected within a given period of time.

Beyond the numerical values, it is important to point out the effectiveness of the representation with respect to the conventional procedures based on all-inclusive coefficients. The proposed solution allows quick evaluations and restores physical meaning to the results achieved. It allows to account for the actual uncertainties (which are different when dealing with a single building, or building aggregates or built-up areas) focusing the role of parameters, seismic demand and other randomness.

References

- Applied Technology Council (1996), *Seismic evaluation and retrofit of concrete buildings*, Report no. ATC-40, Redwood City, California.
- Bal, I.E., Crowley, H. and Pinho, R. (2008), "Displacement-based earthquake loss assessment for an earthquake scenario in Istanbul", *J. Earthq. Eng.*, **12**(1), 12-22.
- Cardone, D. (2007), "Nonlinear static methods vs experimental shaking table test results", *J. Earthq. Eng.*, **11**, 847-975.
- Cattari, S., Curti, E., Giovinazzi, S., Lagomarsino, S., Parodi, S. and Penna, A. (2004), "A mechanical model for the vulnerability assessment and damage scenario of masonry buildings at urban scale", *Proc. 11th Italian Conference on Earthquake Engineering*, Genoa, Italy.
- Cattari, S., Lagomarsino, S. and Parodi, S. (2009), "Formulazione di un modello meccanico per l'analisi di vulnerabilità sismica del costruito in muratura", *Atti del XIII Convegno ANIDIS "L'Ingegneria Sismica in Italia"*, Bologna, Italy, CD-Rom.
- Cattari, S., Lagomarsino, S., Pagnini, L. and Parodi, S. (2010), "Probabilistic seismic damage scenario by mechanical models: the case study of Sulmona (Italy)", *Proc., 14th European Conference on Earthquake Engineering*, Ohrid, Republic of Macedonia.
- Crowley, H., Pinho, R. and Bommer, J.J. (2004), "A probabilistic displacement-based vulnerability assessment procedure for earthquake loss estimation", *Bull. Earthq. Eng.*, **2**(2), 173-219.
- Crowley, H., Bommer, J.J., Pinho, R. and Bird, J. (2005), "The impact of epistemic uncertainty on an earthquake

- loss model”, *Earthq. Eng. Struct. Dyn.*, **34**, 1653-1685.
- D’Ayala, D.F. (2005), “Force and displacement based vulnerability assessment for traditional buildings”, *Bull. Earthq. Eng.*, **3**, 235-265.
- Erberik, M.A. (2008), “Generation of fragility curves for Turkish masonry buildings considering in-plane failure modes”, *Earthq. Eng. Struct. Dyn.*, **37**(3), 387-405.
- Eurocode 8 (2005), *BS EN 1998-1:2005, Design of structures for earthquake resistance. General rules, seismic actions and rules for buildings*, European Committee for Standardization, Brussels.
- Fajfar, P. (1999), “Capacity spectrum method based on inelastic demand spectra”, *Earthq. Eng. Struct. Dyn.*, **28**, 979-993.
- Federal Emergency Management Agency (1997), *NEHRP Guidelines for the seismic rehabilitation of buildings*, FEMA-273, Washington, D.C.
- Freeman, S.A. (1998), “The capacity spectrum method”, *Proc. 11th European Conference on Earthquake Engineering*, Balkema, Paris.
- Haldar, A. and Mahadevan, S. (2000), *Probability, reliability and statistical methods in engineering design*, Wiley, New York.
- HAZUS 99 (1999), *Earthquake loss estimation methodology*, Technical Manual, FEMA, Washington, D.C.
- Lagomarsino, S. and Giovinazzi, S. (2006), “S. Macroseismic and mechanical models for the vulnerability and damage assessment of current buildings”, *Bull. Earthq. Eng.*, **4**, 415-443.
- Lagomarsino, S., Cattari, S., Pagnini, L. and Parodi, S. (2010), *Development of a dynamical model for seismic hazard assessment at national scale*, Report of S2 Project, DPC-INGV 2007-2009.
- Mallardo, V., Malvezzi, R., Milani, E. and Milani, G. (2008), “Seismic vulnerability of historical masonry buildings: a case study in Ferrara”, *Eng. Struct.*, **30**, 2223-2241.
- Restrepo-Velez, L.F. and Magenes, G. (2004), “Simplified procedure for the seismic risk assessment of unreinforced masonry buildings”, *Proc. 13th World Conference on Earthquake Engineering*, Vancouver, Paper No. 2561.
- Rota, M., Penna, A. and Magenes, G. (2010), “A methodology for deriving analytical fragility curves for masonry buildings based on stochastic nonlinear analyses”, *Eng. Struct.*, **32**(5), 1312-1323.
- Turnšek, V. and Čačovič, F. (1971), “Some experimental results on the strength of brick masonry walls”, *SIBMAC Proceedings*, England.
- Vicente, R.V., Varum, H. and Mendes da Silva, J.A.R. (2006), “Vulnerability assessment of traditional buildings in Coimbra, Portugal, supported by a GIS tool”, *Proc First European Conference on Earthquake Engineering and Seismology*, Geneva, Switzerland.